Remote Sensing of Environment 155 (2014) 178–193

Contents lists available at ScienceDirect

Remote Sensing of Environment

journal homepage: www.elsevier.com/locate/rse

Global, Landsat-based forest-cover change from 1990 to 2000

Do-Hyung Kim *, Joseph O. Sexton, Praveen Noojipady, Chengquan Huang, Anupam Anand, Saurabh Channan, Min Feng, John R. Townshend

Global Land Cover Facility, Department of Geographical Sciences, University of Maryland, College Park, MD, USA

ARTICLE INFO

Article history:
Received 24 January 2014
Received in revised form 4 August 2014
Accepted 10 August 2014
Available online 26 September 2014

Keywords:
Forest cover
Landsat
Change detection
Classification

ABSTRACT

Historical baselines of forest cover are needed to understand the causes and consequences of recent changes and to assess the effectiveness of land-use policies. However, historical assessment of the global distribution of forest cover and change has been lacking due to obstacles in image acquisition, computational demands, and lack of retrospective reference data for image classification. As limitations of access to imagery and computational power are overcome, the possibility is increased of an automated retrospective classification of forest cover. We used locally fit classification trees to relate hind-cast observations of "stable pixels" of forest and non-forest cover from circa-2000 to Landsat spectral measurements taken from the circa-1990 epoch of the Global Land Survey collection of Landsat images. Based on analysis of nearly 30,000 Landsat images, forest-cover change between 1990 and 2000 epochs was detected based on joint probabilities of cover in the two epochs. Assessed across a sample of areas with coincident reference data in the conterminous United States, the resulting maps achieved 93% accuracy for forest cover and 84% for forest-cover change—comparable or even higher than many previous national efforts. Global accuracy assessment likewise showed accuracy of 88% for forest-cover change. The maps depict the global distribution of gross gains and losses in forest cover, as well as their net change. The initial analysis showed strong effects of extant land use in temperate regions and land-use change in the tropics over the period, while wildfire dominated in the boreal zone. Regions of high net forest loss (e.g., Amazonia) were associated with land-use changes into agriculture, and regions of high gross gains and losses (e.g., southeastern US, Sweden) were associated with intensive forestry. These results, including the global forest cover and forest cover change datasets, will be a basis for the estimation of the efficacy of policies and analyzing correlation between forest cover change and socio-economic factors.

1. Introduction

1.1. Background

Climatological and anthropogenic factors are causing widespread changes in Earth's forest cover. Since the public opening of the USGS Landsat archive (Woodcock et al., 2008), there have been efforts to report global forest-cover and its changes at the 30-meter resolution of the Landsat sensors. Most of these efforts have concentrated on recent changes (2000–present) (Hansen et al., 2013; Sexton et al., 2013a; Townshend et al., 2012). However, historical baselines are needed to understand the causes and consequences of these changes and to assess the effectiveness of land-use policies, most notably for Reducing Emissions from Deforestation and Degradation (REDD) (Olander, Gibbs, Steininger, Swenson, & Murray, 2008).

Consistent with the United Nations Framework Convention on Climate Change (UNFCCC, 2002), United Nations Food and Agriculture Organization (FAO, 2006), and International Geosphere–Biosphere Programme (Belward, 1996), here the term "forest cover" refers to a specified density of trees, and not to land use as pertaining to forestry (Hansen, Stehman, & Potapov, 2010; Di Gregorio & Jansen, 2000). The term "cover" itself generalizes binary (presence vs. absence) as well as continuous (e.g., percent) scales of representation. Forests and forest cover thus defined are relevant to ecosystem processes such as chemical (e.g., carbon) and hydrological cycling, energy budgets, and biodiversity, whereas other definitions might be more applicable to socio-economic phenomena such as land tenure.

Most land-cover changes are small in area, and regional patterns develop over long (e.g., decadal) time scales (Lambin, Geist, & Lepers, 2003; Townshend & Justice, 1988). Consequently, effective monitoring requires longer-term data sets with fine spatial resolution—ideally at sub-hectare spatial resolutions spanning multiple decades (Sexton, Urban, Donohue, & Song, 2013b; Townshend & Justice, 1988). Further, the precision of analyses based on these data depends upon consistency of the definition of "forest" versus "non-forest" over space and time (Sexton, Urban, Donohue, & Song, 2013b). Several geospatial data sets represent Earth's forest cover globally (e.g. Hansen, DeFries, Townshend, & Sohlberg, 2000, Hansen et al., 2013; Loveland et al., 2000; Potapov et al., 2008; Sexton, Song, et al., 2013a), but none have both the spatial

* Corresponding author.
E-mail address: rsgis@umd.edu (D.-H. Kim).

http://dx.doi.org/10.1016/j.rse.2014.08.017

and temporal scale required for longer-term (i.e., pre-2000), global monitoring of forest-cover change at fine spatial resolution.

Provision of appropriately scaled data has in the past been hindered by two constraints: (1) access to large volumes of satellite imagery and (2) the coincident reference observations required to translate image pixels into estimates of cover. Given their global coverage, spatial resolution (30- to 60-m), and temporal extent (1972–present), the archive of Landsat data is the best source of information for retrieving historical baselines of forest cover (Olander et al., 2008; Townshend & Justice, 1988). But whereas the 2009 opening of the USGS Landsat archive has released the constraint of data access, retrospective mapping of forest cover is still limited by a lack of coincident reference data required for supervised image classifications.

1.2. Objectives

We demonstrate the feasibility of extending global, Landsat-resolution mapping and change detection to 1990. We present a method to retrieve historical maps of forest cover and change from 1990 to 2000 based on archival Landsat images and reference data hind-cast from more recent (i.e., post-2000) periods. We report the first results of this retrospective classification and change-detection algorithm, including: (1) a map of circa-1990 forest cover at 30-m resolution and global extent with a correspondingly scaled layer estimating classification uncertainty and (2) a global map of forest-cover change between circa-1990 and -2000, also with a corresponding uncertainty layer. To assess the quality of the forest-cover and -change estimates, we report error estimates relative to samples of independent reference data collected over the United States and globally, and we compare these validation results to those from previous change-detection efforts. Given the sensitivity of empirical classifiers, special attention is paid to assess the efficacy of methods and to minimize the impact of sampling bias.

2. Methods

2.1. Data and processing

2.1.1. Landsat-based surface reflectance

Landsat images from the 1990 Global Land Survey (GLS) collection (Gutman et al., 2008) were the primary source of imagery of the 1990 "epoch". Representing conditions around the nominal years of 1975, 1990, 2000, 2005, and 2010, the GLS was selected to optimize cloud-free conditions during the growing season for land-cover change studies. The 1990 epoch ranges from 1984 to 1997; images were taken preferentially from years near the target year 1990, but images far from 1990 were chosen by necessity in cloudy or otherwise poorly sampled regions. GLS coverage over the high northern latitudes and over western India and the surrounding region was prevented by gaps in the USGS archive. Also, nearly half of the original GLS-1990 dataset did not have correct radiometric gain and bias coefficients at the time of data acquisition; thus atmospheric correction and conversion to surface reflectance were not possible (Chander, Markham, & Helder, 2009; Chander et al., 2004; Townshend et al., 2012). These uncalibrated GLS images were replaced after the original GLS compilation with substitutes from the updated USGS archive within the epoch wherever possible (Fig. 2). To perform the selection of replacement imagery while minimizing phenological or atmospheric noise, a tool was constructed to query the USGS Global Visualization Viewer (GloVis) database (glovis.usgs.gov/) for appropriate images based on

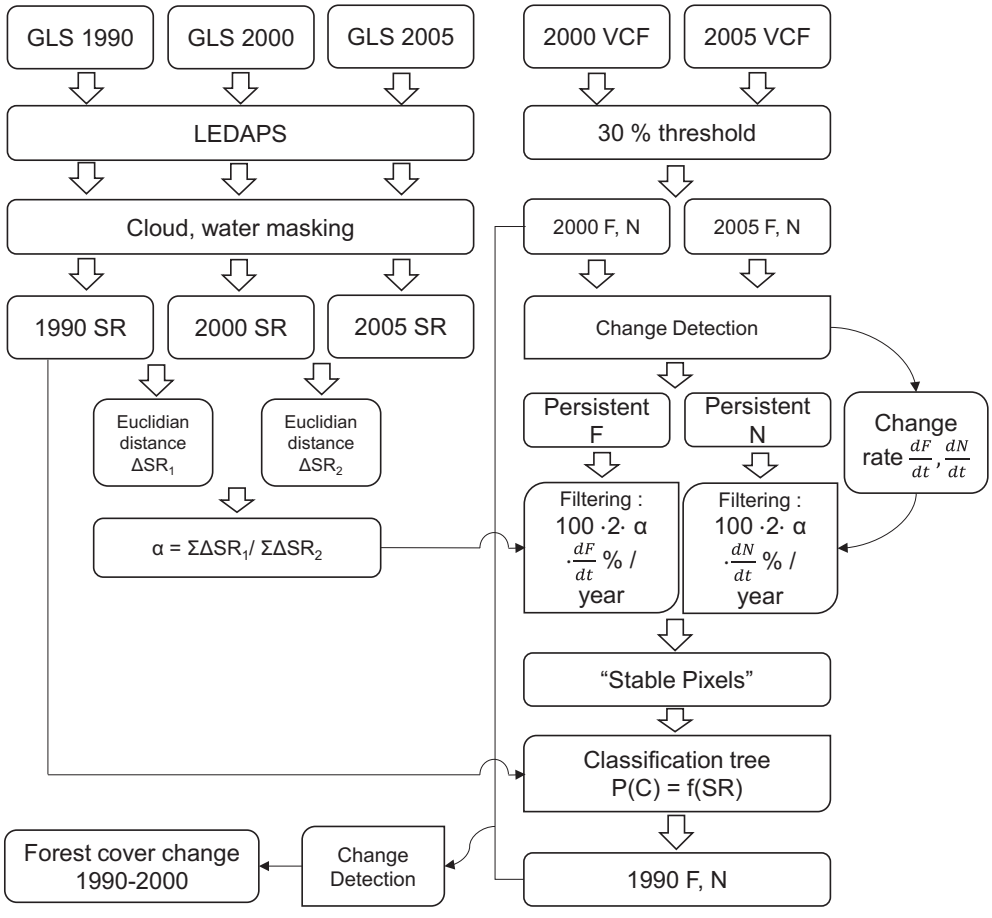

Fig. 1. Hind-cast training and classification procedure to retrieve historical forest cover estimates. SR = surface reflectance, C = cover, $t_1 \approx 1990$, and $tn \approx 2000$ or 20005.

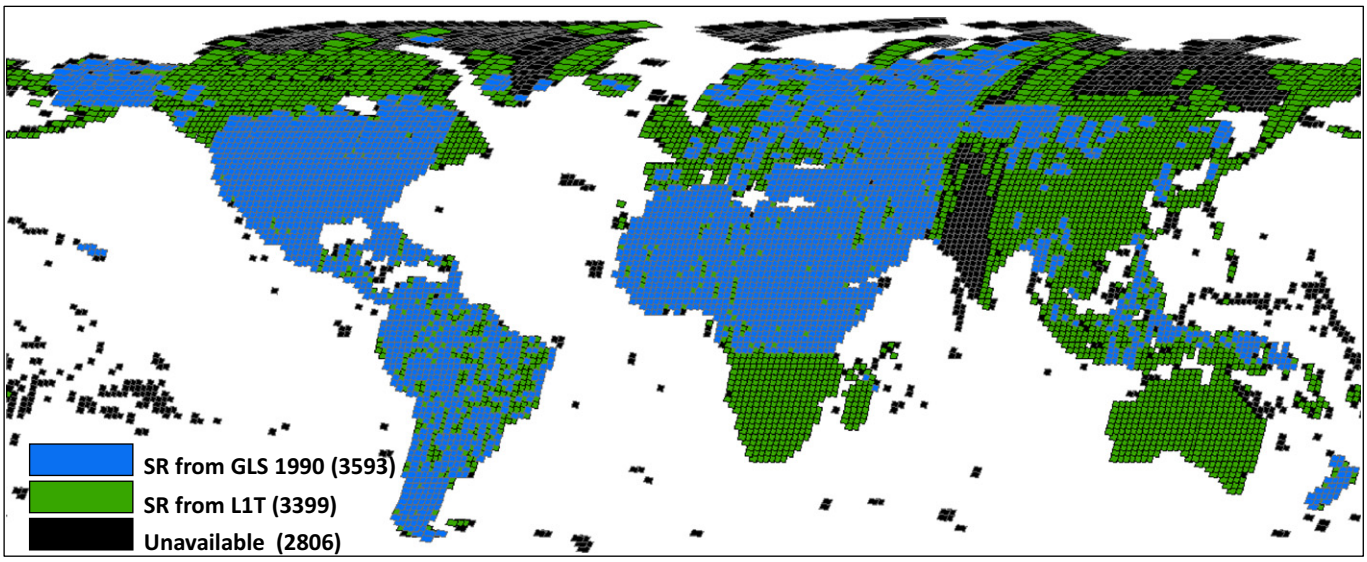

Fig. 2. Sources of calibrated Landsat images for estimating surface reflectance (SR). Blue tiles represent SR images from the 1990 Global Land Survey collection of Landsat images, and green tiles represent SR images from downloaded L1T images. Black tiles represent areas with no available data in the USGS archive for the 1990 epoch (1984–1997).

phenological time series of Normalized Difference Vegetation Index (NDVI) from the MODerate-resolution Spectroradiometer (MODIS) (Kim, Narashiman, Sexton, Huang, & Townshend, 2011; Townshend et al., 2012).

Each image of this enhanced GLS dataset was then atmospherically corrected to surface reflectance using the Landsat Ecosystem Disturbance Adaptive Processing System (LEDAPS) (Masek et al., 2006). The surface reflectance data set from the enhanced version of GLS-1990 is available from the Global Land Cover Facility (www.landcover.org) and use of these data is strongly recommended for studies based on the GLS-1990 data. Clouds were identified in a spectral-temperature space (Huang et al., 2010a) and removed from subsequent analysis. This "aggressive" cloud-detection algorithm's low rate of omission error makes it suitable for masking pixels from forest-cover change analysis. Cloud shadows were identified by projecting cloud masks onto a digital elevation model through solar geometry at the time of image acquisition (Huang et al., 2010a) and were also removed from analysis.

2.1.2. Forest cover maps in 2000 and 2005 GLS epochs

We used tree-cover and error estimates from a global, Landsat-based tree-cover dataset for 2000 and 2005 GLS epochs (Sexton, Song, et al., 2013a) available from the Global Land Cover Facility (www.landcover.org). Following the International Geosphere–Biosphere Programme (IGBP) definition of forests (Townshend, 1992), forest cover maps for 2000 and 2005 epochs were derived by imposing a 30% threshold of tree-cover for discriminating forest from non-forest. Forest-cover change maps between 2000 and 2005 epochs were derived by image differencing (Sexton et al., *in press*; data available at www.landcover.org). The overall global accuracy was approximately 89%. More details on accuracy assessment are presented in the Results section.

2.2. Forest-cover retrieval using stable pixels

For the purpose of large-area mapping, extrapolation of models beyond the immediate temporal and spatial domain in which they were trained has been explored by many researchers (e.g., Botkin, Estes, MacDonald, & Wilson, 1984; Gray & Song, 2013; Pax-Lenney, Woodcock, Macomber, Gopal, & Song, 2001; Sexton, Urban, Donohue, & Song, 2013b; Woodcock, Macomber, Pax-Lenney, & Cohen, 2001). Termed as "generalization" or "signature extension", this approach to extend spectral signatures through time and space has been successfully applied for the classification of forest cover (Pax-Lenney et al., 2001) and change (Woodcock et al., 2001) using Landsat data. This approach has been implemented by deriving training data from one date and using it to train a classifier on a different image from the same path/row scene but different acquisition date (Pax-Lenney et al., 2001). Complementary to the traditional signature extension method, Gray and Song (2013) combined a procedure to identify stable pixels to deal with irregular time-series images. This approach has been found to be effective for the automated classification of large areas, especially when there are actual changes in class spectral signatures from phenological variability, atmospheric differences, or land cover changes (Fortier, Rogan, Woodcock, & Miller Runfola, 2011; Gray & Song, 2013).

2.2.1. Reference forest/non-forest data

Persistent forest (F) and non-forest pixels (N) were sampled from forest-cover change maps between 2000 and 2005 GLS epochs and then filtered so that only "stable" pixels—i.e., those whose class did not change between 1990 and 2000 epochs—were retained for analysis. The details of the filtering process are presented below.

For each WRS-2 scene, an annual rate of forest-cover (F) change, $\frac{dF}{dt}$, and an annual rate of non-forest-cover (N) change, $\frac{dN}{dt}$, were calculated as:

$$\frac{dF}{dt} = \frac{|F_{t2} - F_{t1}|}{t2 - t1} \quad (1)$$

$$\frac{dN}{dt} = \frac{|N_{t2} - N_{t1}|}{t2 - t1} \quad (2)$$

where F and N are the percentage of forest and non-forest pixels, respectively, and t_1 and t_2 were respectively the acquisition years of the Landsat images for 2000 and 2005 GLS epochs.

The spectral difference (ΔSR) – quantified as the Euclidean distance between two pixels over time in the spectral domain – was calculated for 1990–2000 (ΔSR_1) and 2000–2005 (ΔSR_2). To minimize impact from accelerating or decelerating rates of forest-cover change between the two periods, a parameter α was defined as the ratio of the sums of spectral difference of all persistent pixels and was calculated as:

$$\alpha = \Sigma\Delta SR_1 / \Sigma\Delta SR_2. \quad (3)$$

Given the large number of available pixels within the overlapping portion of two Landsat images within the same WRS-2 scene, α was doubled to increase the selectivity of filtering for stable pixels. A percentage of forest equaling $\alpha \times 2 \times 100 \times \frac{dF}{dt}$ and non-forest pixels equaling $\alpha \times 2 \times 100 \times \frac{dN}{dt}$ were thus removed per year of difference between 1990- and 2000-epoch images in the order of spectral difference (ΔSR). Limiting the sample to pixels that were stable from 2000 to 2005 minimized inclusion of erroneous data, and filtering the most spectrally different pixels from 1990 to the later epochs removed the pixels most likely to have changed over that period (Fig. 3). A positive relationship between given α for each scene and estimated change between 1990 and 2000 epoch for selected WRS-2 scenes is demonstrated in Appendix A (Fig. A1).

2.2.2. Forest cover classification

Using the sample of stable-pixel locations, a forest/non-forest reference sample was extracted from forest-cover maps in 2000 and 2005. This sample was then filtered to maximize certainty and minimize change between observation periods (Fig. 1).

Forest cover in circa-1990 was retrieved by a classification-tree algorithm. The probability of forest cover, $p(F)$, in each pixel i at time $t \approx 1990$ was estimated by a conditional relationship (g) to remotely sensed covariates (X):

$$\hat{p}(F)_{i,t} = g\left(X_{i,t}\right), \tag{4}$$

where X is a vector of surface reflectance and temperature estimates; subscripts i and t denote the pixel's location in space, indexed by pixel, and time indexed by year. The relation g was parameterized using the C5.0™ classification-tree software (Quinlan, 1986), trained on a sample of pixels within each Landsat image; the model was thus fit locally within each Landsat World Reference System 2 (WRS-2) scene. Reflectance and temperature covariates were acquired from the 1990-epoch Global Land Survey collection of Landsat images (Gutman et al., 2008) and other Landsat images selected from the USGS archive, each of which was atmospherically corrected to surface reflectance and converted to radiant temperature by the LEDAPS implementation of the 6S radiative transfer algorithm (Masek et al., 2006). Whereas retrievals from within the period of overlap between the Landsat-5, Landsat-7, and MODIS eras may be based on general—even global—models based on phenological metrics that require dense image samples within each year (e.g., Hansen et al., 2013), this local fitting instead maximizes use of the single-image coverage characteristic of much of the history of Earth observation. Use of atmospherically corrected surface reflectance fulfills the conditions for signature extension in space (Pax-Lenney et al., 2001; Woodcock et al., 2001).

2.3. Forest-cover change

Classification trees estimate the probability $p(C)$ of each class in each pixel as a conditional relative frequency. Given $C =$ "F" (i.e., "forest"), each pixel was labeled either "forest" or "non-forest" based on $p(F)$:

$$F \stackrel{\text{def}}{=} p(F) \geq 0.5 \tag{5}$$

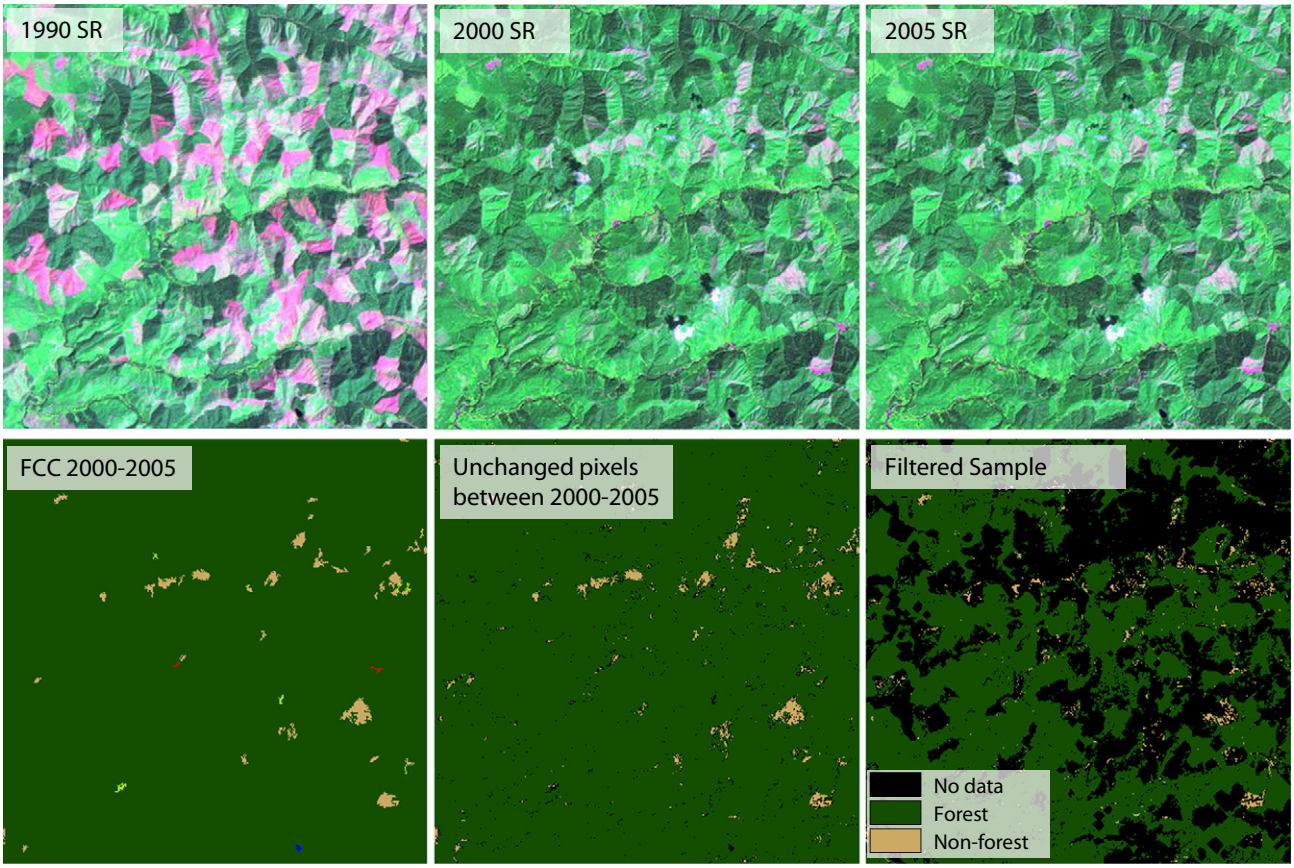

Fig. 3. Example of training data selection from existing forest covers data (path 47, row 27). Upper three 7, 4, and 2 band composite images are surface reflectance from Landsat images acquired for the 1990, 2000 and 2005 epochs respectively. The lower left image is forest cover change map from the 2000 to 2005 epoch, the central lower image depicts only persistent forest and non-forest samples selected from 2000 to 2005 change map and the right-hand image in the lower row is the final training data after the filtering procedure based on surface reflectance covariance.

$$N \stackrel{\text{def}}{=} p(F) < 0.5. \quad (6)$$

Forest-cover change between 1990 and 2000 epochs was detected given the joint probabilities in 1990 and 2000 epochs (Sexton, in press):

$$p(FF_i) = p(F_{it1}) \times p(F_{it2}) \quad (7)$$

$$p(NN_i) = (1-p(F_{it1})) \times (1-p(F_{it2})) \quad (8)$$

$$p(NF_i) = (1-p(F_{it1})) \times p(F_{it2}) \quad (9)$$

$$p(FN_i) = p(F_{it1}) \times (1-p(F_{it2})) \,. \quad (10)$$

That is, given the probability of forest p(F) vs. non-forest p(N) in a pixel i in the 1990-epoch (t_1) and 2000-epoch (t_2), four classes were derived: stable forest (*FF*), stable non-forest (*NN*), forest gain (*NF*), and forest loss (*FN*). A categorical map of change classes was then produced by assigning each pixel the class with the highest probability.

2.4. Weighting

Decision trees and other empirical classifiers are sensitive to bias in training samples relative to class proportions within their population of inference (Borak, 1999; Carpenter, Gopal, Macomber, Martens, & Woodcock, 1999; Sexton, Urban, Donohue, & Song, 2013b; Song, 2010; Woodcock et al., 2001) and to uncertainty in the training data set (McIver & Friedl, 2002; Strahler, 1980). To minimize these effects, we maintained a large sample with representative class proportions by removing a small, but equal fraction of the least stable pixels from each class while maintaining the class proportions from reference epoch to training sample. Further, we weighted each pixel's contribution to the classifier's parameterization based on the pixel's classification certainty in the reference data. A weight w was adopted for each pixel as the classification probability of the estimate ($p_{\max}$) of forest- or non-forest cover (C) from the 2000-epoch dataset:

$$W_i = p_{\max}(C_i). \quad (11)$$

The weights were then applied to adjust the objective (i.e., purity) function maximized by the iterative binary recursion algorithm employed by C5.0™ (Quinlan, 1986).

2.5. Accuracy assessment

2.5.1. Accuracy assessment for the conterminous United States

A sample of nine Landsat World Reference System 2 (WRS-2) scenes across the conterminous United States was selected to assess the accuracy of 1990 forest-cover and 1990–2000 forest-cover change estimates (Fig. 4). These scenes were originally used as reference data for the North American Forest Disturbance (NAFD) program of the North American Carbon Program. Collection of reference data for accuracy assessment was described by Thomas et al. (2011). A design-based, stratified random sample for the four classes of forest cover change detection (*FF*, *NN*, *NF* and *FN*) was gathered to represent rare change classes (*FN* and *NF*) as well as the more common stable classes (*FF* and *NN*). Stratification was based on initial classes identified by the Vegetation Change Tracker algorithm (VCT) (Huang et al., 2010b), and selection probabilities were used to remove sampling biases in the error matrix. Each sample pixel was examined by expert interpreters and labeled as changed or persistent forest/non-forest pixel after a visual evaluation of Landsat time series imagery and high resolution imagery from TerraServer (www.terraserver.com) and/or Google Earth (www.earth.google.com). Knowledge of the spectral properties, temporal changes, and spatial context of the pixel within the context of the surrounding landscape over time was used together to label each sample pixel.

2.5.2. Global accuracy assessment

Global accuracy was estimated based on a confusion matrix between collected reference data and the forest-cover change detection results. Similar to the NAFD assessment, sampling bias at the scene level as well as at individual pixels was corrected by assigning weights based on inclusion probability (Stehman, Wickham, Smith, & Yang, 2003). Global accuracy assessment was performed using reference data collected from 89 WRS-II tiles (Fig. 4). These sites were selected using a stratified random sampling scheme to represent major biomes identified by Olson et al. (2001). Sampling and response design were similar to those of the NAFD protocol used for the US accuracy assessment.

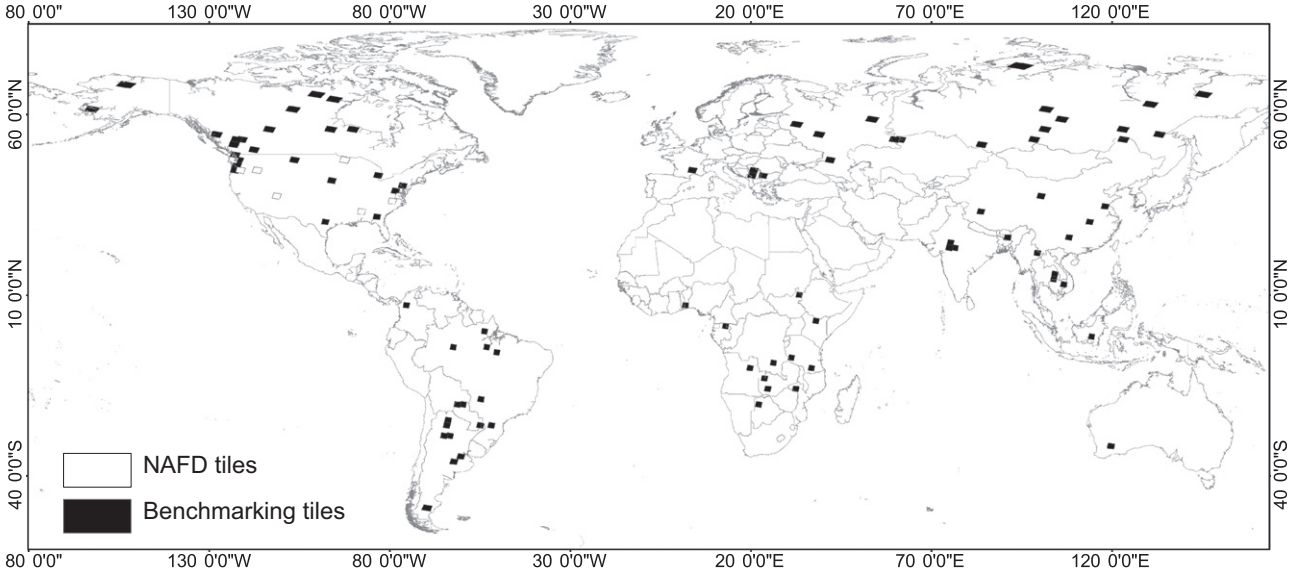

Fig. 4. Landsat WRS-2 tiles used for error assessment including 9 NAFD tiles (Thomas et al., 2011) and 89 tiles for global accuracy assessment.

The number of observations per scene varied between 350 and 625, totaling >25,000 samples globally. Each observation was labeled as either forest or non-forest for each epoch, including 1990, 2000, and 2005, using a web-based forest-change labeling tool (Feng et al., 2012). This tool facilitates rapid labeling of forest cover and change using fine-resolution imagery automatically co-registered to multi-temporal Landsat images.

3. Results and discussion

3.1. Accuracy assessment for the conterminous United States

3.1.1. Accuracy of forest cover maps

Accuracy estimates for the 1990 global forest cover map ("FC 1990") relative to the NAFD sample are presented in Table 1. For precedent, accuracy estimates comparing the US 1992 National Land Cover Database (NLCD 1992) against the NAFD sample are included in parentheses. The average accuracy and kappa coefficient of FC 1990 for all 9 WRS-2 tiles were 93% and 0.72, demonstrating a strong relationship between the reference data and classified maps overall. The FC 1990 map was the most accurate in areas dominated by closed-canopy forest (e.g., WRS-2 path 16, row 35, path 45, row 29 and path 47, row 27) but had comparatively low accuracy in sparsely forested areas (e.g., path 37, row 34). The FC 1990 was slightly biased toward the "forest" class, with errors of commission toward forest greater than those toward non-forest. Overall, the FC 1990 map showed higher accuracy than NLCD 1992, with only one exception in sparse forests (path 37, row 34).

Weighting the training sample proportional to certainty had a positive effect on accuracy of the final estimates. Accuracy of forest cover maps estimated from un-weighted training data was 88.57%, approximately 3% lower than those derived from weighted training data (Appendix A). Improvement in accuracy was greatest in path 47, row 27, where forests are characterized by dense, tall trees, and lowest in path 37, row 34, characterized by short and sparse woody vegetation.

3.1.2. Accuracy of forest cover change map

Compared against the NAFD reference data, the FCC 1990–2000 forest-change map showed similar or even higher accuracy than the NLCD change product. Our change map had the greatest accuracy in persistent forest and non-forest classes and had accuracy comparable to the NLCD change product in forest gain and loss classes. Accuracy of the FCC 1990–2000 forest cover change map and spatially corresponding NLCD 1992–2001 Retrofit Land Cover Change Product is presented in Table 2.

Overall accuracy of FCC 1990–2000 for all nine NAFD sites was 83%, and average kappa coefficient was 0.64—greater than the NLCD change product by 7% and 0.14, respectively. Similar to the accuracy of the forest cover maps, the accuracy of the forest cover change map was higher in closed-canopy forest (WRS-II path 16, row 35, path 45, row 29, and path 47, row 27) and lower in sparsely forested areas (e.g., path 37, row 34). Omission errors were slightly less than commission errors in the persistent forest class. With the exception of path 37, row 34, commission errors in persistent forest ranged from 1.5% to 16% while omission error ranged from 2.4% to 19%. Most errors in persistent forest were from misclassification of forest loss as persistent forest. These errors have been attributed to sub-pixel scale disturbance such as partial or non-stand clearing (Thomas et al., 2011). Errors committed to persistent non-forest (9–40%) were more frequent than errors committed to persistent forest. Path 27, row 27 had the largest commission error rate, mainly caused by confusion between wetland and forest, which was also observed in the NAFD assessment (Thomas et al., 2011). The omission error rate of persistent non-forest was less than that of persistent forest, ranging from 0 to 12.2% with the exception of path 37, row 34. The rate of commission error to forest loss was 34% and to forest gain was 32% across all 9 NAFD sites. For both forest change classes, omission from persistent forest class was the largest source of error.

3.2. Global accuracy assessment

The overall accuracy for the 2000–2005 forest cover change map was about 89% globally (Table 3), and the overall accuracy for the 1990–2000 forest cover change map was approximately 88% (Table 4). We also report the accuracy of the results for 1990–2000 by major forest biomes (Appendix A). Among the forest biomes, tropical evergreen forest and temperate evergreen forest showed the highest accuracy of 95 and 90%, respectively, while tropical deciduous forest showed the lowest accuracy, 70% (Appendix A).

This pattern of uncertainty, also evident in the global distribution of classification and change-detection certainty (Fig. 5), suggests that the global distribution of classification and change-detection certainty was driven primarily by the density and height of tree cover. Dense forests in the tropics and temperate zones were associated with relatively high classification certainty, and treeless deserts (e.g., central Australia

Table 1
Accuracy assessment of (static) forest and non-forest classes. Accuracy estimates for the 1990 forest cover map were based on reference data from North American Forest Disturbance (NAFD) program (Thomas et al., 2011). For comparison, accuracy estimates from coincident data taken from the US 1990 National Land Cover Database (NLCD 1992) are included in parentheses.

p045r029	Kappa		0.65 (0.41)	p012r031	Kappa		0.78 (0.57)	p021r037	Kappa		0.76 (0.36)
	N	*F*			*N*	*F*			*N*	*F*	
N	**14 (16)**	3 (28)	82.4 (36.4) %	*N*	**82 (93)**	5 (71)	94.3 (56.7)	*N*	**176 (115)**	12 (66)	93.6 (63.6)
F	11 (9)	**350 (325)**	97 (97.3)%	*F*	31 (21)	**452 (390)**	93.6 (94.9)	*F*	53 (118)	**432 (379)**	89.1 (76.3)
	56 (64)%	99.1 (92)%	**96.3 (90.2)%**		72.6 (81.6)	98.9 (84.6)	**93.7 (84)**		76.9 (49.4)	97.3 (85.2)	**90.3 (72.9)**
p047r027	Kappa		0.81 (0.62)	p015r034	Kappa		0.76 (0.39)	p027r027	Kappa		0.63 (0.45)
	N	*F*			*N*	*F*			*N*	*F*	
N	**34 (27)**	1 (8)	97.1 (77.1)	*N*	**143 (96)**	40 (80)	78.1 (54.6)	*N*	**57 (75)**	5 (80)	91.9 (48.4)
F	14 (21)	**527 (525)**	97.4 (96.2)	*F*	18 (66)	**369 (331)**	95.4 (83.4)	*F*	49 (32)	**438 (366)**	89.9 (92)
	70.1 (56.2)	99.8 (98.5)	**97.4 (95.1)**		88.8 (59.2)	90.2 (80.5)	**89.8 (74.5)**		53.8 (70.1)	98.9 (82.1)	**90.2 (79.8)**
p042r029	Kappa		0.85 (0.82)	p016r035	Kappa		0.87 (0.5)	p037r034	Kappa		0.38 (0.52)
	N	*F*			*N*	*F*			*N*	*F*	
N	**94 (93)**	13 (15)	87.9 (86.1)	*N*	**70 (53)**	15 (61)	82.4 (46.5)	*N*	**84 (43)**	86 (6)	55.9 (87.8)
F	10 (14)	**248 (278)**	96.1 (95.2)	*F*	4 (21)	**624 (579)**	99.4 (96.5)	*F*	2 (47)	**122 (206)**	81.4 (81.4)
	90.4 (87)	95 (95)	**93.7 (92.8)**		94.6 (71.6)	97.7 (90.4)	**97.3 (88.5)**		62.6 (47.8)	76.8 (92.2)	**72.3 (82.5)**

Table 2
Accuracy assessment of forest-cover change. Accuracy estimates for the 1990–2000 forest cover change map were based on reference data from North American Forest Disturbance (NAFD) program (Thomas et al., 2011). For comparison, accuracy estimates from coincident data taken from the NLCD 1992/2001 Retrofit Land Cover Change Product are included in parentheses.

p045r029	Kappa 0.6 (0.57)				
	NN	*NF*	*FN*	*FF*	%
NN	**14** (17)	0 (0)	0 (14)	0 (3)	100 (50)
NF	0 (0)	**0** (0)	1 (0)	1 (0)	0 (0)
FN	0 (0)	0 (0)	**7** (5)	2 (10)	77.8 (33)
FF	4 (1)	3 (3)	14 (3)	**201** (191)	90.5 (96)
%	77.8 (94)	0 (0)	31.8 (23)	98.5 (94)	**90** (86)

p012r031	Kappa 0.74 (0.53)				
	NN	*NF*	*FN*	*FF*	
NN	**67 (87)**	0 (1)	1 (31)	0 (60)	98.5 (49)
NF	8 (0)	**3** (0)	0 (0)	4 (2)	20 (0)
FN	16 (9)	1 (0)	**83** (52)	12 (14)	74.1 (69)
FF	10 (6)	3 (6)	20 (22)	**302** (245)	90.2 (88)
	66.3 (85)	42.9 (0)	79.8 (50)	95 (76)	**85.9** (72)

p021r037	Kappa 0.69 (0.31)				
	NN	*NF*	*FN*	*FF*	
NN	**97 (96)**	3 (2)	0 (38)	0 (69)	97 (47)
NF	8 (1)	**67** (14)	0 (0)	10 (3)	78.8 (78)
FN	9 (1)	0 (0)	**58** (14)	26 (13)	62.4 (50)
FF	3 (21)	41 (95)	30 (36)	**315** (266)	81 (64)
	82.9 (81)	60.4 (13)	66 (16)	89.7 (76)	**80.5** (58)

p047r027	Kappa 0.58 (0.36)				
	NN	*NF*	*FN*	*FF*	
NN	**28 (30)**	0 (1)	0 (14)	1 (42)	96.6 (35)
NF	1 (0)	**5** (0)	0 (0)	0 (1)	83.3 (0)
FN	0 (0)	0 (0)	**7** (2)	6 (2)	53.8 (50)
FF	2 (1)	11 (15)	29 (20)	**318** (285)	88.3 (89)
	90.3 (97)	31.3 (0)	19.4 (6)	97.9 (57)	**87.8** (77)

p015r034	Kappa 0.69 (0.44)				
	NN	*NF*	*FN*	*FF*	
NN	**79 (79)**	4 (3)	3 (22)	4 (35)	87.8 (57)
NF	4 (0)	**54** (2)	0 (0)	32 (1)	60 (67)
FN	3 (1)	0 (1)	**38** (18)	18 (7)	64.4 (67)
FF	6 (12)	8 (60)	21 (23)	**273** (284)	88.6 (75)
	85.9 (86)	81.8 (3)	61.3 (29)	84 (87)	**81.2** (70)

p027r027	Kappa 0.47 (0.22)				
	NN	*NF*	*FN*	*FF*	
NN	**29 (43)**	3 (13)	0 (21)	0 (55)	90.6 (33)
NF	4 (3)	**16** (6)	1 (6)	4 (6)	66.7 (29)
FN	7 (0)	0 (0)	**46** (1)	21 (1)	39.1 (50)
FF	25 (20)	15 (15)	55 (74)	**267** (232)	81.7 (68)
	44.6 (65)	47.1 (18)	45.1 (1)	91.4 (79)	**72.6** (57)

p042r029	Kappa 0.77 (73)				
	NN	*NF*	*FN*	*FF*	
NN	**83 (81)**	2 (0)	1 (4)	7 (11)	89.3 (84)
NF	1 (0)	**0** (0)	0 (0)	0 (0)	0 (0)
FN	2 (1)	0 (0)	**9** (6)	8 (0)	47.4 (86)
FF	5 (12)	0 (2)	6 (8)	**123** (148)	91.8 (87)
	91.2 (86)	0 (0)	56.2 (33)	89.1 (93)	**87** (86)

p016r035	Kappa 0.8 (0.6)				
	NN	*NF*	*FN*	*FF*	
NN	**64 (63)**	0 (0)	1 (8)	1 (47)	94.1 (53)
NF	2 (0)	**4** (0)	0 (0)	11 (8)	23.5 (0)
FN	1 (2)	0 (0)	**21** (17)	12 (5)	61.8 (70)
FF	3 (5)	0 (4)	8 (5)	**449** (413)	97.6 (97)
	91.4 (90)	100 (0)	70 (56)	94.9 (87)	**93.2** (85)

p037r034	Kappa 0.38 (0.81)				
	NN	*NF*	*FN*	*FF*	
NN	**74** (67)	1 (0)	0 (0)	64 (2)	53.2 (97)
NF	4 (0)	**0** (0)	0 (0)	13 (0)	0 (0)
FN	0 (3)	0 (0)	**0** (0)	3 (0)	– (–)
FF	2 (14)	0 (1)	0 (0)	**81** (163)	97.6 (92)
	92.5 (80)	0 (0)	– (–)	50.3 (99)	**64** (92)

Table 3
Global accuracy of forest cover change maps for 2000–2005 epoch. The global scale accuracy was estimated based on a confusion matrix between reference data collected from 89 WRS-II tiles and the forest cover change detection results. Similar to the NAFD assessment, sampling bias at the scene level as well as at individual pixels was corrected by assigning weight based on inclusion probability.

		Change map						
		FF	*FN*	*NF*	*NN*	Total (n)	Samples	Producer's accuracy
Reference	*FF*	0.35	0.00	0.00	0.09	0.45	13,562	0.78
	FN	0.00	0.00	0.00	0.00	0.01	1632	0.48
	NF	0.00	0.00	0.00	0.00	0.01	933	0.20
	NN	0.00	0.00	0.00	0.53	0.54	10,624	0.99
	Total	0.36	0.01	0.00	0.63	1.00	26,751	
User's accuracy		0.98	0.50	0.32	0.84		Overall:	**0.89**

and the Sahara desert), grasslands (e.g., Mongolia and Patagonia), and tundra (e.g., Northern Canada) also showed very high certainty of non-forest cover. However, sparse and/or short forests, such as the boreal forests of North America and Eurasia, the Sahelian and Miombo woodlands of Africa, and the Chaco and Atlantic dry forests of South America, were associated with relatively low certainty in the forest/non-forest classification. Anthropogenically fragmented forests in ecologically productive regions—e.g., the southeastern United States, southeastern China and eastern Brazil—were mapped with intermediate certainty.

3.2.1. Sources of confusion in semi-arid regions

In spite of the overall efficacy of the algorithm, the Utah site (path 37, row 34) showed comparatively low accuracy for both forest cover and change maps. Located in a semi-arid, mountainous, sparsely vegetated region, forest signatures here could be confused by terrain shadowing and understory vegetation, which varies in space and time in response to rainfall and temperature (Thomas et al., 2011). The gradient of height and cover of woody vegetation also likely resulted in semantic confusion between shrubs vs. trees and between forests vs. savannas (Sexton, Song, et al., 2013a).

3.2.2. Visual assessment of forest cover change map

The regional drivers of forest dynamics were readily observable in the 1990–2000 forest-cover change map. Fig. 6 shows examples of visual assessments observed within our accuracy assessment sites. Forest cover changes in path 21, row 37 (Mississippi) and path 47, row 27 (Oregon) are characterized by even-aged silviculture of evergreen needle-leaf trees, including clear-cut harvesting. Small clearings due to urbanization were the dominant pattern in path 12, row 31 (New England) and path 27, row 27 (Minnesota), where wind damage and timber harvest dominated losses (Huang et al., 2010; Thomas et al., 2011).

Table 4
Global accuracy of forest cover change maps for 1990–2000 epoch.

		Change map						
		FF	*FN*	*NF*	*NN*	Total (n)	Samples	Producer's accuracy
Reference	*FF*	0.34	0.01	0.01	0.07	0.43	12,876	0.80
	FN	0.00	0.01	0.00	0.01	0.01	1956	0.45
	NF	0.00	0.00	0.00	0.02	0.03	1583	0.16
	NN	0.00	0.00	0.00	0.52	0.53	9153	0.99
	Total	0.35	0.02	0.01	0.62	1.00	25,568	
User's accuracy		0.97	0.39	0.28	0.85		Overall:	**0.88**

3.2.3. Improvement by sample weighting

Weighting based on input classification certainty (as classification probability) improved accuracy by ~3%. Weighting was more effective at minimizing the influence of uncertain training data in patchily heterogeneous landscapes, but less effective in landscapes comprising continuous gradients of woody vegetation height and cover. Accuracy increases due to weighting were highest in the Oregon site (path 47, row 27), characterized by tall, dense forests with extensive logging and regrowth, and were lowest in the Utah site (path 37, row 34), characterized by low, sparse forest and relatively low anthropogenic forest-cover change rates. The scene-level mean uncertainty (RMSE) of the 2000-epoch Landsat tree-cover layer (Sexton, Song, et al., 2013a) at path 47, row 27 was 12.55%-about ten times higher than the scene-level mean uncertainty of 1.28% at path 37, row 34. Although there appears to be a limit to which such weighting schemes can improve accuracy, the improvements are encouraging. Increasing the classification accuracy of heterogeneous landscapes is considered among the most challenging tasks for improving global land cover mapping (Gong et al., 2013; Herold, Mayaux, Woodcock, Baccini, & Schmullius, 2008). We expect that, where sample selection criteria are less effective at filtering unstable pixels, weighting the sample based on prior certainty can contribute modest improvements in accuracy.

3.3. Global, circa-1990 distribution of forest cover, change, and uncertainty

Fig. 7 demonstrates the feasibility of extending global, Landsat-resolution mapping and change detection to 1990. Several studies have described recent, i.e., post-2000, global patterns of forest cover and change (Gong et al., 2013; Hansen et al., 2013), and others have noted regional patterns of forest loss prior to 2000 (Achard et al., 2002, 2005, 2006, 2014; Bodart et al., 2013; DeFries et al., 2002; Ernst et al., 2013; Eva et al., 2012; Mayaux et al., 2005, 2013; Stibig, Achard, Carboni, Raši, & Miettinen, 2014; Hansen et al., 2009). Except for gaps remaining due to data availability, our results extend the historical record of Earth's forest cover to the previous decade and globally.

The global distribution of forest cover in 1990 was similar to that reported for subsequent years (Hansen et al., 2000, 2013; Loveland et al., 2000; Mayaux et al., 2005, 2013; Potapov et al., 2008; Sexton, Song, et al., 2013a) (Fig. 8). Although the global distribution continues to be constrained primarily by climate, the fine-scale changes responsible for altering that distribution over time were predominantly anthropogenic. The land-use effect was strongest in temperate and tropical regions over the period, while wildfire dominated in the boreal zone. Regions of high net forest loss (e.g., Amazonia) were associated with land-use changes from wilderness to agriculture, and regions of high gross gains and losses (e.g., southeastern US) were associated with intensive forestry. These generalities are discussed in the following paragraphs. Quantitative discussion of observed changes will be the subject of subsequent papers. However, we do note several instances of the various trajectories of change from the last decade of the 20th century to the first decade of the 21st: (i) long-term forest stability, (ii) gains and/or losses continuing steadily from the previous decade into the next, and (iii) acceleration of change between the decades.

Remote regions that exhibited little forest change in the first decade of the 21st century also experienced stability in the previous decade. The most stable forests from 1990 to 2000 tended to be those which were both at the core of their climatological regions as well as distant from human pressure. The central Amazon and Congo basins were relatively undisturbed, experiencing neither large losses nor gains as a fraction of their respective areas. This was also true for some part of boreal forest in Northern Canada and Russia. Even regions in relatively close proximity to areas of harvest and regeneration or to conversion of forests to other land uses—i.e., the Appalachian mountains of the eastern US, highlands of southeastern Asia—exhibited relatively low rates of disturbance and regrowth.

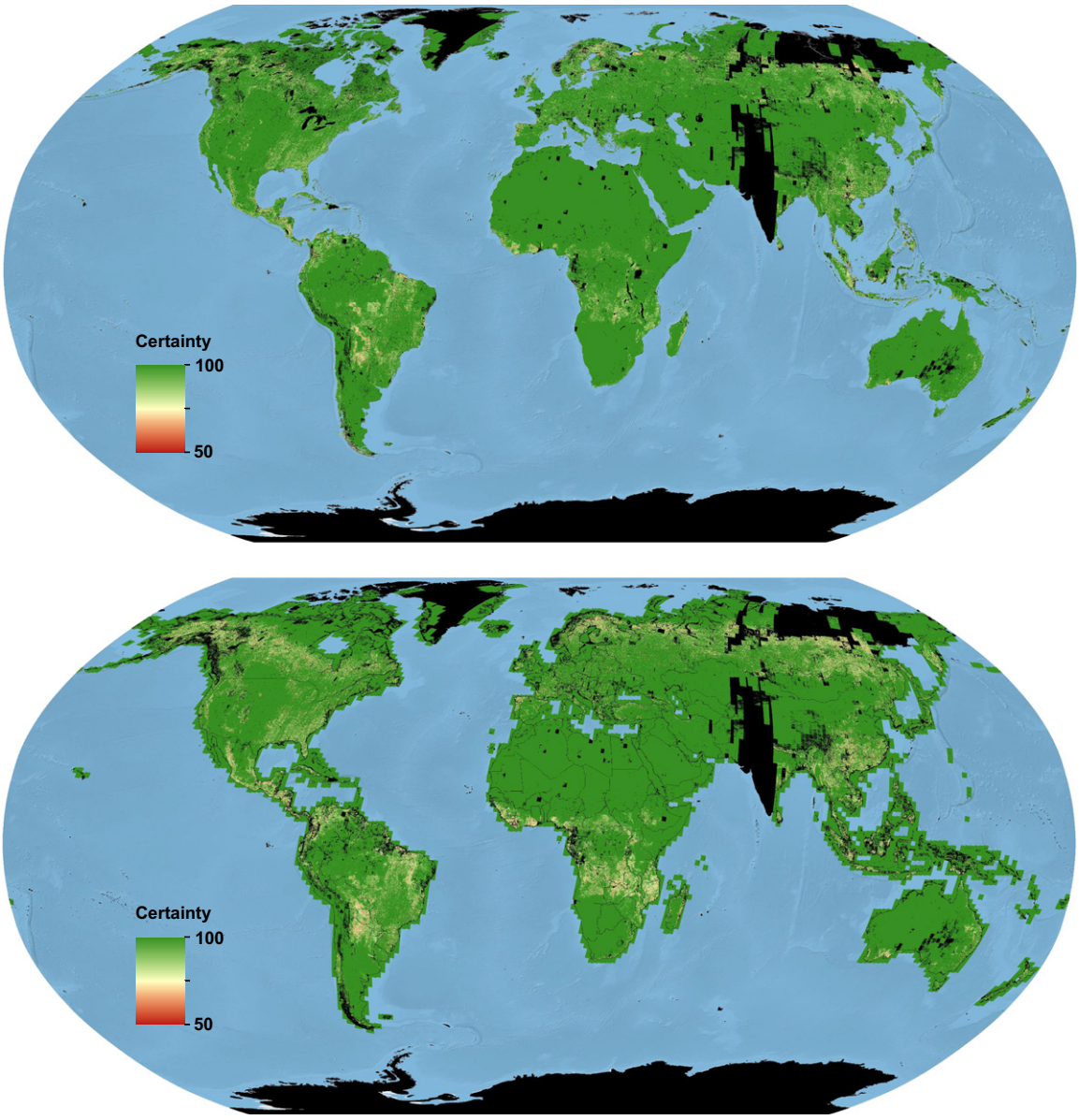

Fig. 5. Global distribution of classification certainty of forest cover (top) and forest-cover change (bottom).

Many areas in temperate and boreal zones that were known to have experienced change in the 21st century were already showing major changes in the 1990s. In the boreal zone, including northern Canada, Europe, and Russia, extensive wildfires were the dominant driver of forest cover change. These disturbances were characterized by large patches of loss with no apparent relation to roads or other human infrastructure. This extends the findings of Pan et al. (2010), who attributed these losses to fire and of Hansen et al. (2010), who attributed the region's losses to both fire and pathogens. In the temperate zone, the greatest changes were due to intensive forestry. For example, subtropical forests in the southeastern U.S. showed notable gains and losses from 1990 to 2000, corroborating previous studies that found high gross gains and losses but relatively low net change in this region (Masek et al., 2008; Sleeter et al., 2013) (Fig. 9A). In this region, pulp- and timber-production were becoming increasingly dominant at the time due to shifting of the American timber industry from the Pacific Northwest region following listing of the Northern Spotted Owl as "Threatened" under the US Endangered Species Act in 1990 and the subsequent passing of the Northwest Forest Plan in 1994. Similarly, intensive forestry was also apparent in Northern Europe, including Southern Sweden (Fig. 9D) and Finland over the period. Widespread changes were found over Sweden and Finland, corroborating previous studies (Achard et al., 2005, 2006). In these regions, forest gain and loss were in close spatial proximity due to intensive regional forest-management practices (Achard et al., 2006; Hansen et al., 2013; Loman, 2010; Ylitalo, 2010).

Many areas that underwent forest clearing in both decades exhibited changing rates of clearing around the turn of the century. In the tropics, losses were by majority due to changes in land use from wilderness to agriculture, which was impacted by shifting economic and conservation policies. Although recent studies have reported decreasing rates of forest-cover loss in the Brazilian Amazon resulting from policies to slow deforestation (Hansen et al., 2013; Nepstad et al., 2014; Souza et al., 2013), the 1990s cover the period of rapid deforestation prior to

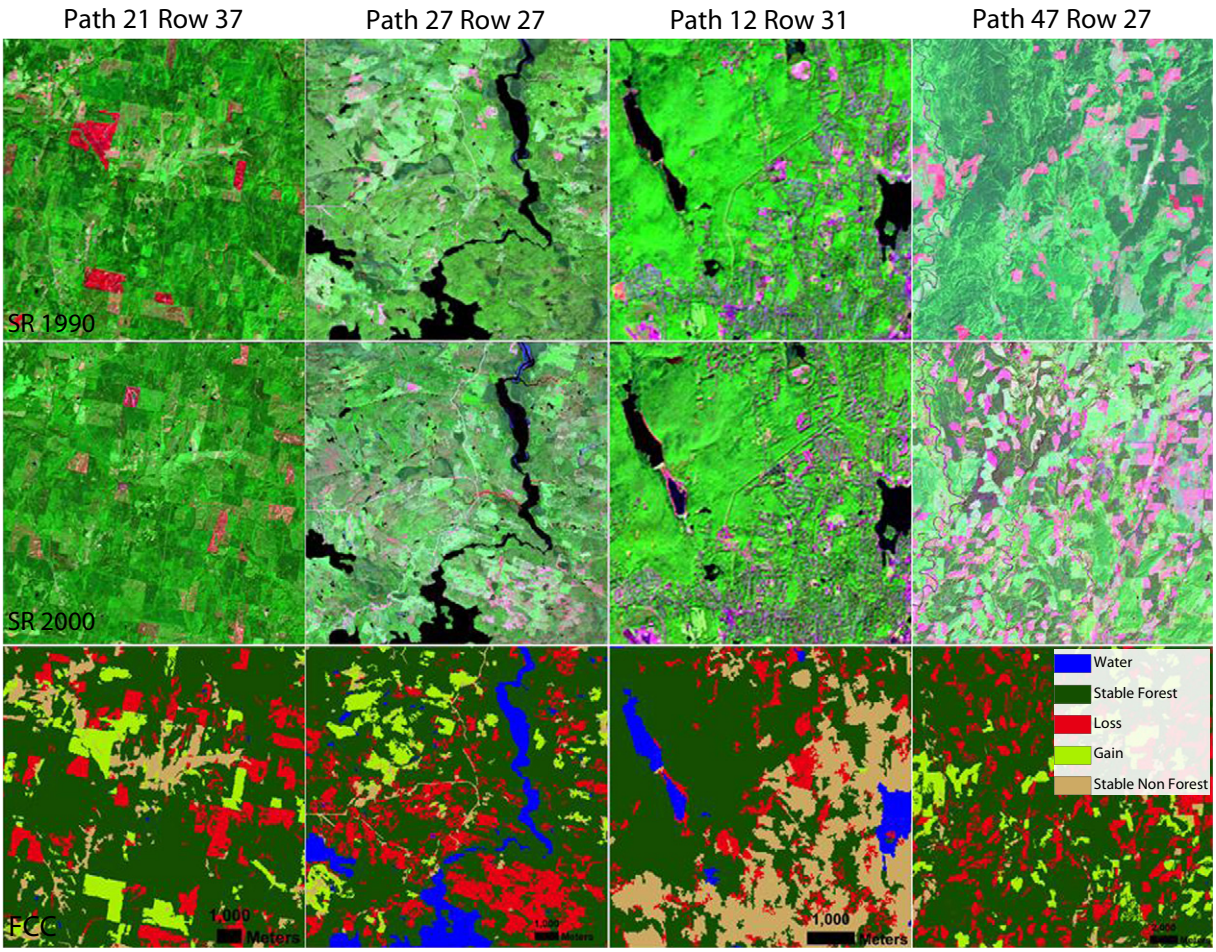

Fig. 6. Visual examination of forest cover change; the top and middle rows of each column are the surface reflectance composites (SWIR2, NIR, G) from the 1990 and 2000 epochs, and the bottom row is the corresponding forest cover change map. Pixels with pink and green hues in the SR images represent bare soil and vegetation, respectively.

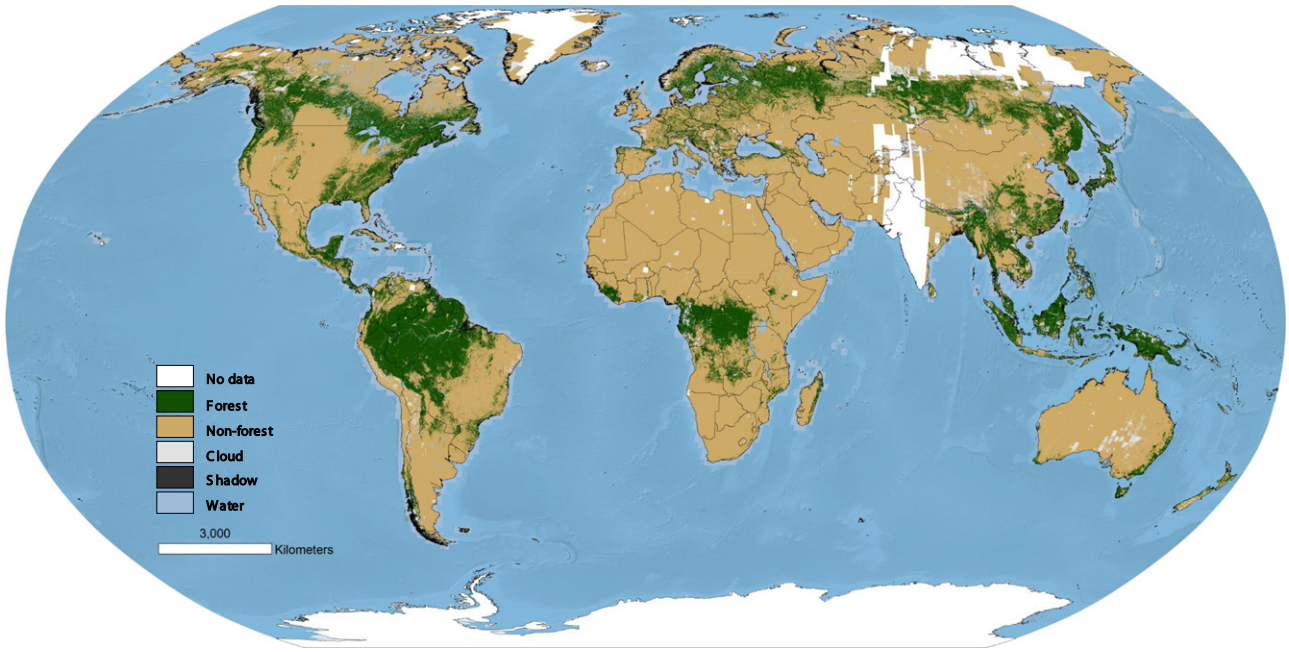

Fig. 7. Global distribution of forest cover, circa-1990.

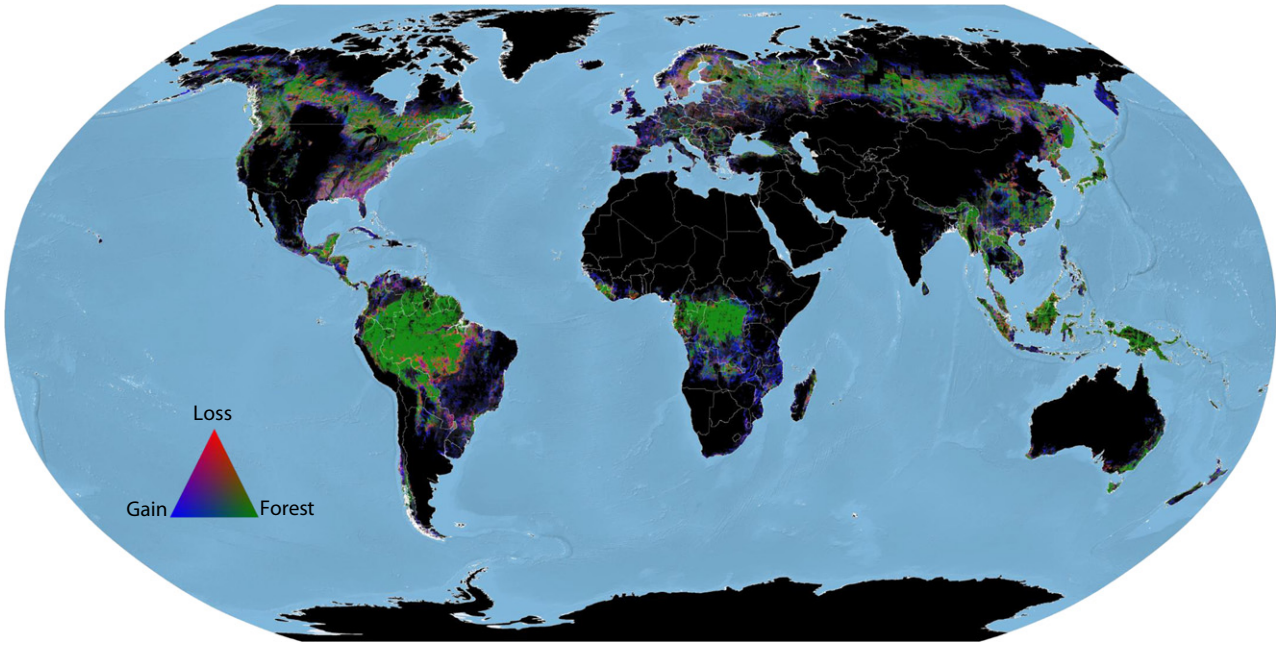

Fig. 8. Global distribution of forest-cover change, circa-1990 to -2000. The false-color composite was aggregated from 30-m to 5-km grid cells. Forest loss is represented in red, forest gain in blue and persistent forest in green. Colors are stretch in the proportion of 1 (forest): 4 (gain): 4 (loss).

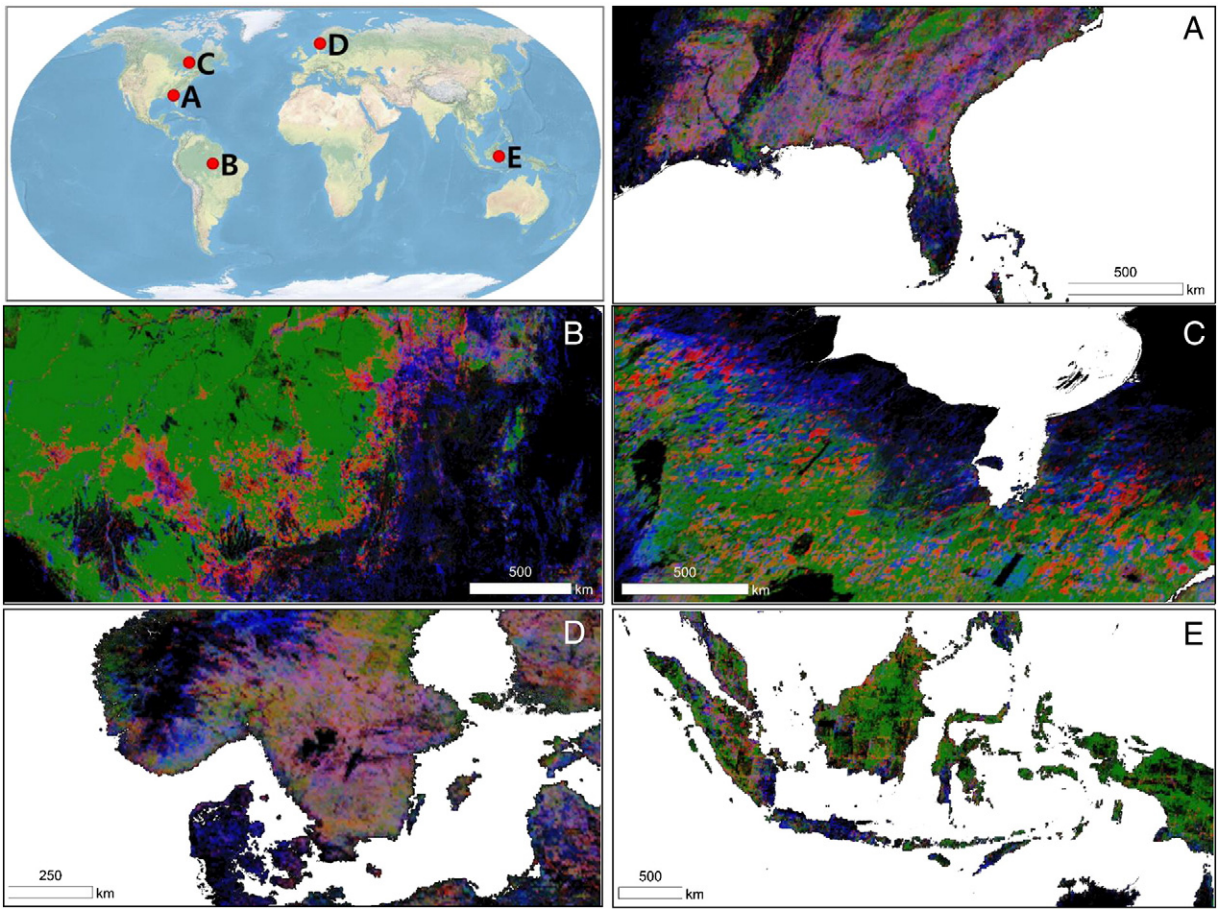

Fig. 9. Regional forest-cover change in: (A) the Southeastern United States, (B) Amazon Basin, (C) Northern Canada, (D) Southern Sweden, and (E) Indonesia.

the policies' enactment (Fig. 9B) when clearing was mainly due to expansion of large-scale cattle ranching (Gibbs et al., 2010; Kanninen et al., 2007). Likewise, although observations over much of Indonesia and the Malaysian archipelago were obscured by clouds, the forest losses of the region appear to have been relatively large, including the expansion of oil palm plantations over the 1990–2000 period before a sharp drop in losses in the early 2000s (Hansen et al., 2009). Conversely, in inland Southeast Asia, including Thailand, Vietnam and Cambodia, our results show much lower deforestation rates than post-2000 period, in contrast to FAO estimates (FAO, 2010) showing rather monotonic forest cover change trends between the two periods. Although Africa shows overall low rates of forest cover change, the Democratic Republic of Congo shows the highest forest cover loss among the African countries, showing elevated deforestation rate later on which may suggest the expansion of agro-industry in this region.

4. Conclusions

We have produced a global map of circa-1990 forest cover and circa-1990 to -2000 forest-cover change from the USGS archive of Landsat images, using training data hind-cast from the 2000 and 2005 Global Land Survey (GLS) epochs. With overall accuracies for the US of 93% for circa-1990 forest cover in 1990 and 84% for circa-1990 to -2000 forest-cover change, the maps are of equal or greater accuracy than 1992–2001 retrofit change product of the 2001 US National Land Cover Database over the conterminous United States. Globally, forest-cover change accuracy was 88%. Our method gained its strength from the use of stable pixels over time and from the minimization of influence from training data uncertainty. Given their slow rate, and thus poor detectability, forest gains were less apparent than were losses.

The maps depict the global distribution of gross gains and losses in forest cover, as well as their net change. Whereas some regions (e.g., the Amazonian arc of deforestation, Indonesia) have been perennial centers of forest loss and others (e.g., the southeastern United States and southern Sweden) have retained relatively rapid rates of both gains and losses from 1990 to 2000. While some regions (e.g. inland Southeast Asian countries) exhibiting rapid change of deforestation rates around 2000, most of Africa exhibited persistent and relatively slow rates of forest cover change except for some regions (e.g. Democratic Republic of Congo).

These findings will be important for inferring the efficacy of policies and for analyzing causal relationship between socio-economic drivers and forest cover changes. The global forest cover and change maps will be made available for free download at the Global Land Cover Facility (www.landcover.org).

Acknowledgments

This work was performed in service of the Global Forest Cover Change Project (www.forestcover.org), a partnership of the University of Maryland Global Land Cover Facility (www.landcover.org) and NASA Goddard Space Flight Center. Funding support for this study was provided by the following NASA programs: Making Earth System Data Records for Use in Research Environments (NNH06ZDA001N-MEASURES), Land Cover and Land Use Change (NNH07ZDA001N-LCLUC), and Earth System Science Research Using Data and Products from Terra, Aqua, and Acrimsat Satellites (NNH06ZDA001N-EOS). The GLS datasets were sent to GLCF by Rachel Headley (USGS). This work was performed at the Global Land Cover Facility.

Appendix A

Table A1
047027 1990–2000 error matrix (normalized).

	Change image						Producer's accuracy	n
		FF	*FN*	*NF*	*NN*	Total		
Field data	*FF*	0.60	0.00	0.00	0.00	0.61	0.98	324
	FN	0.02	0.01	0.00	0.00	0.03	0.39	36
	NF	0.04	0.00	0.01	0.00	0.05	0.24	16
	NN	0.01	0.00	0.00	0.29	0.31	0.95	69
	Total	0.67	0.01	0.02	0.30	1.00		445
User's accuracy		0.90	0.80	0.58	0.99	Overall accuracy	0.92	

Table A2
045029 1990–2000 error matrix (normalized).

	Change image						Producer's accuracy	n
		FF	*FN*	*NF*	*NN*	Total		
Field data	*FF*	0.80	0.00	0.00	0.01	0.81	0.99	204
	FN	0.01	0.01	0.00	0.00	0.02	0.57	22
	NF	0.01	0.00	0.00	0.00	0.01	0.00	3
	NN	0.03	0.00	0.00	0.13	0.16	0.80	19
	Total	0.85	0.01	0.00	0.14	1.00		248
User's accuracy		0.94	0.90	0.00	0.93	Overall accuracy	0.94	

Table A3
042029 1990–2000 error matrix (normalized).

	Change image						Producer's accuracy	n
		FF	*FN*	*NF*	*NN*	Total		
Field data	*FF*	0.33	0.01	0.00	0.03	0.38	0.87	137
	FN	0.00	0.01	0.00	0.00	0.01	0.64	16
	NF	0.00	0.00	0.00	0.00	0.00	0.00	2
	NN	0.01	0.01	0.00	0.59	0.61	0.97	93
	Total	0.34	0.03	0.00	0.63	1.00		248
User's accuracy		0.96	0.24		0.94	Overall accuracy	0.93	

Table A4
037034 1990–2000 error matrix (normalized).

	Change image						Producer's accuracy	n
		FF	*FN*	*NF*	*NN*	Total		
Field data	*FF*	0.07	0.05	0.00	0.33	0.45	0.16	160
	FN	0.00	0.00	0.00	0.00	0.00		0
	NF	0.00	0.00	0.00	0.00	0.00	0.00	1
	NN	0.00	0.00	0.00	0.55	0.55	1.00	81
	Total	0.07	0.05	0.00	0.88	1.00		242
User's accuracy		1.00	0.00	0.00	0.63	Overall accuracy	0.62	

Table A5
027027 1990–2000 error matrix (normalized).

	Change image						Producer's accuracy	n
		FF	*FN*	*NF*	*NN*	Total		
Field data	*FF*	0.53	0.02	0.00	0.00	0.55	0.96	293
	FN	0.09	0.03	0.00	0.00	0.12	0.25	103
	NF	0.01	0.00	0.01	0.01	0.03	0.44	34
	NN	0.04	0.01	0.01	0.23	0.30	0.78	93
	Total	0.67	0.06	0.03	0.24	1.00		523
User's accuracy		0.79	0.51	0.47	0.96	Overall accuracy	0.80	

Table A6
021037 1990–2000 error matrix (normalized).

	Change image						Producer's accuracy	n
		FF	*FN*	*NF*	*NN*	Total		
Field data	*FF*	0.43	0.03	0.01	0.01	0.48	0.91	351
	FN	0.04	0.06	0.00	0.00	0.10	0.57	89
	NF	0.06	0.00	0.06	0.01	0.13	0.48	111
	NN	0.02	0.01	0.02	0.26	0.29	0.87	131
	Total	0.55	0.09	0.09	0.27	1.00		682
User's accuracy		0.79	0.61	0.74	0.93	Overall accuracy	0.81	

Table A7
016035 1990–2000 error matrix (normalized).

	Change image						Producer's accuracy	n
		FF	*FN*	*NF*	*NN*	Total		
Field data	*FF*	0.66	0.01	0.01	0.00	0.69	0.96	470
	FN	0.00	0.02	0.00	0.00	0.02	0.71	29
	NF	0.00	0.00	0.00	0.00	0.00	1.00	4
	NN	0.00	0.00	0.01	0.27	0.28	0.94	78
	Total	0.67	0.03	0.02	0.27	1.00		581
User's accuracy		0.99	0.48	0.17	0.98	Overall accuracy	0.95	

Table A8
015034 1990–2000 error matrix (normalized).

	Change image						Producer's accuracy	n
		FF	*FN*	*NF*	*NN*	Total		
Field data	*FF*	0.50	0.02	0.03	0.02	0.56	0.89	327
	FN	0.03	0.04	0.00	0.01	0.08	0.54	64
	NF	0.01	0.00	0.05	0.00	0.06	0.79	66
	NN	0.01	0.00	0.00	0.29	0.31	0.95	118
	Total	0.54	0.06	0.07	0.33	1.00		575
User's accuracy		0.91	0.72	0.65	0.89	Overall accuracy	0.88	

Table A9
012031 1990–2000 error matrix (normalized).

	Change image						Producer's accuracy	n
		FF	*FN*	*NF*	*NN*	Total		
Field data	*FF*	0.36	0.00	0.00	0.01	0.37	0.96	321
	FN	0.01	0.03	0.00	0.00	0.05	0.73	104
	NF	0.00	0.00	0.00	0.00	0.01	0.23	7
	NN	0.04	0.01	0.01	0.50	0.57	0.88	180
	Total	0.42	0.05	0.01	0.51	1.00		612
User's accuracy		0.86	0.67	0.17	0.98	Overall accuracy	0.90	

Table A10
Normalized overall accuracy of FCC 1990–2000 for nine NAFD sites.

	Change image						Producer's accuracy	n
		FF	*FN*	*NF*	*NN*	Total		
Field data	*FF*	0.40	0.02	0.01	0.09	0.51	0.77	2587
	FN	0.02	0.02	0.00	0.00	0.05	0.49	463
	NF	0.01	0.00	0.02	0.00	0.03	0.49	244
	NN	0.02	0.00	0.01	0.38	0.41	0.93	862
	Total	0.45	0.05	0.03	0.47	1.00		4156
User's accuracy		0.88	0.46	0.60	0.80	Overall accuracy	0.81	

Table A11
Accuracy measurement of FC 1990 without being weighted by certainty for training pixels.

p045r029	Kappa		0.65 (0.41)	p012r031	Kappa		0.78 (0.57)	p021r037	Kappa		0.76 (0.36)
	N	*F*	Producer's (%)		*N*	*F*			*N*	*F*	
N	173	3	98.29	*N*	228	1	99.56	*N*	215	6	97.28
F	32	105	76.64	*F*	21	38	64.40	*F*	25	93	78.81
User's (%)	84.39	97.22	88.81		91.56	97.43	92.36		89.58	93.93	90.85
p047r027	Kappa		0.81 (0.62)	p015r034	Kappa		0.76 (0.39)	p027r027	Kappa		0.63 (0.45)
	N	*F*			*N*	*F*			*N*	*F*	
N	265	1	99.62	*N*	187	18	91.21	*N*	223	2	99.11
F	37	62	62.62	*F*	10	72	87.80	*F*	45	55	55
	87.74	98.41	89.58		94.92	80	90.24		83.20	96.49	85.53
p042r029	Kappa		0.85 (0.82)	p016r035	Kappa		0.87 (0.5)	p037r034	Kappa		0.38 (0.52)
	N	*F*			*N*	*F*			*N*	*F*	
N	125	5	96.15	*N*	316	4	98.75	*N*	60	42	58.82
F	20	172	89.58	*F*	17	75	81.52	*F*	36	147	80.32
	86.20	97.17	92.23		94.89	94.93	94.90		62.5	77.77	72.63

Table A12
Global accuracy of forest cover change maps for 1990–2000 by biomes.

	Image	*FF*	*FN*	*NF*	*NN*	TotalC	ProdAccu
Boreal forest	Reference						
	FF	0.61	0.03	0.02	0.08	0.73	0.83
	FN	0.01	0.01	0.00	0.00	0.02	0.45
	NF	0.01	0.00	0.01	0.01	0.03	0.37
	NN	0.01	0.00	0.00	0.20	0.22	0.94
	TotalR	0.63	0.04	0.03	0.30	1.00	NA
	UsersAccu	0.96	0.22	0.39	0.67	Overall	0.83
Temperate deciduous forest	Reference						
	FF	0.30	0.01	0.01	0.03	0.35	0.86
	FN	0.00	0.00	0.00	0.01	0.02	0.26
	NF	0.00	0.00	0.00	0.05	0.05	0.04
	NN	0.01	0.00	0.00	0.57	0.58	0.98
	TotalR	0.31	0.01	0.01	0.66	1.00	NA
	UsersAccu	0.96	0.35	0.16	0.86	Overall	0.88
Temperate evergreen forest	Reference						
	FF	0.61	0.01	0.01	0.02	0.65	0.93
	FN	0.00	0.02	0.00	0.00	0.03	0.80
	NF	0.01	0.00	0.02	0.01	0.05	0.39
	NN	0.01	0.01	0.01	0.24	0.27	0.90
	TotalR	0.64	0.04	0.04	0.28	1.00	NA
	UsersAccu	0.95	0.56	0.46	0.88	Overall	0.90
Tropical deciduous forest	Reference						
	FF	0.34	0.01	0.01	0.21	0.57	0.60
	FN	0.00	0.01	0.00	0.02	0.03	0.36
	NF	0.01	0.00	0.00	0.04	0.05	0.04
	NN	0.00	0.00	0.00	0.35	0.35	0.98
	TotalR	0.35	0.02	0.01	0.61	1.00	NA
	UsersAccu	0.97	0.44	0.18	0.56	Overall	0.70
Tropical evergreen forest	Reference						
	FF	0.81	0.01	0.01	0.01	0.84	0.97
	FN	0.00	0.01	0.00	0.00	0.02	0.68
	NF	0.00	0.00	0.00	0.01	0.02	0.27
	NN	0.00	0.00	0.00	0.11	0.12	0.94
	TotalR	0.83	0.03	0.01	0.14	1.00	NA
	UsersAccu	0.99	0.58	0.38	0.83	Overall	0.95

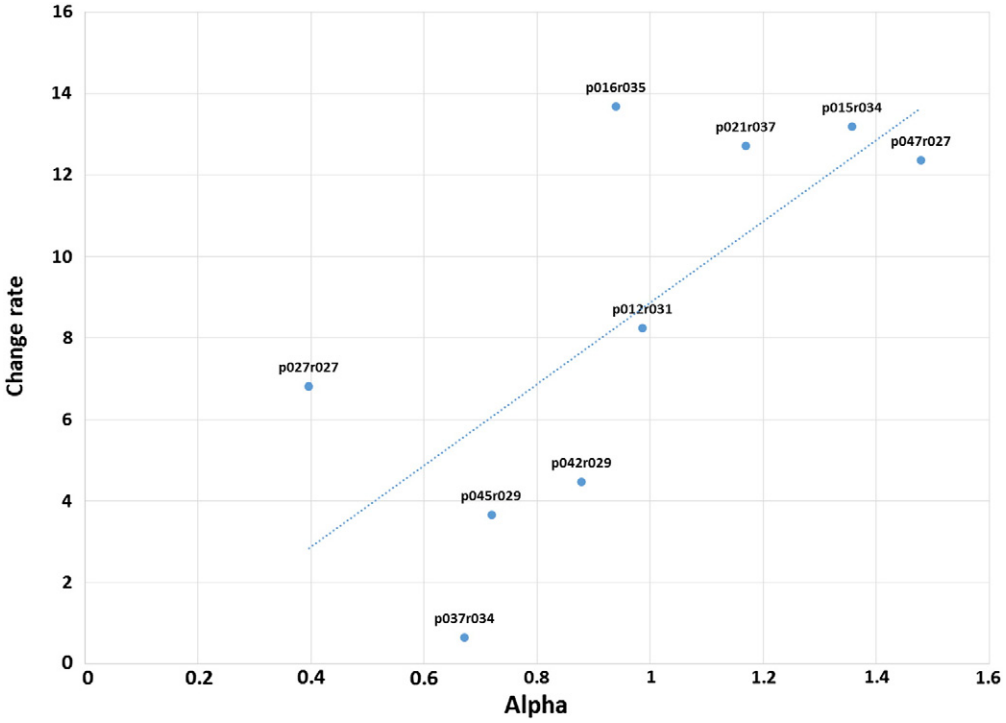

Fig. A1. The relationship between alpha, the ratio of the sums of spectral difference of all persistent pixels and change rate between 1990 and 2000 epochs for persistent pixels.

References

Achard, F., Beuchle, R., Mayaux, P., Stibig, H. J., Bodart, C., Brink, A., et al. (2014). Determination of tropical deforestation rates and related carbon losses from 1990 to 2010. *Global Change Biology*, *20*(9), 2841–2855.

Achard, F., Eva, H. D., Stibig, H. J., Mayaux, P., Gallego, J., Richards, T., et al. (2002). Determination of deforestation rates of the world's humid tropical forests. *Science*, *297*(5583), 999–1002.

Achard, F., Mollicone, D., Stibig, H. J., Aksenov, D., Laestadius, L., Li, Z., et al. (2006). Areas of rapid forest-cover change in boreal Eurasia. *Forest Ecology and Management*, *237*(1), 322–334.

Achard, F., Stibig, H. J., Laestadius, L., Roshchanka, V., Yaroshenko, A., & Aksenov, D. (2005). *Identification of "hot spot areas" of forest cover changes in boreal Eurasia*. Office for Official Publications of the European Communities.

Belward, A. S. (1996). The IGBP-DIS global 1 km land cover data set "DISCover": Proposal and implementation plans. *Report of the Land Cover Working Group of IGBP-DIS*. Toulouse: IGBP-DIS Office.

Bodart, C., Brink, A. B., Donnay, F., Lupi, A., Mayaux, P., & Achard, F. (2013). Continental estimates of forest cover and forest cover changes in the dry ecosystems of Africa between 1990 and 2000. *Journal of Biogeography*, *40*(6), 1036–1047.

Borak, J. S. (1999). Feature selection and land cover classification of a MODIS-like data set for a semiarid environment. *International Journal of Remote Sensing*, *20*(5), 919–938.

Botkin, D. B., Estes, J. E., MacDonald, R. M., & Wilson, M. V. (1984). Studying the Earth's vegetation from space. *BioScience*, *508–514*.

Carpenter, G. A., Gopal, S., Macomber, S., Martens, S., & Woodcock, C. E. (1999). A neural network method for mixture estimation for vegetation mapping. *Remote Sensing of Environment*, *70*(2), 138–152.

Chander, G., Helder, D. L., Markham, B.L., Dewald, J.D., Kaita, E., Thome, K. J., et al. (2004). Landsat-5 TM reflective-band absolute radiometric calibration. *IEEE Transactions on Geoscience and Remote Sensing*, *42*(12), 2747–2760.

Chander, G., Markham, B.L., & Helder, D. L. (2009). Summary of current radiometric calibration coefficients for Landsat MSS, TM, ETM+, and EO-1 ALI sensors. *Remote Sensing of Environment*, *113*(5), 893–903.

DeFries, R. S., Houghton, R. A., Hansen, M. C., Field, C. B., Skole, D., & Townshend, J. (2002). Carbon emissions from tropical deforestation and regrowth based on satellite observations for the 1980s and 1990s. *Proceedings of the National Academy of Sciences*, *99*(22), 14256–14261.

Di Gregorio, A., & Jansen, L. J. M. (2000). *Land Cover Classification System (LCCS): Classification Concepts and User Manual*. FAO.

Ernst, C., Mayaux, P., Verhegghen, A., Bodart, C., Christophe, M., & Defourny, P. (2013). National forest cover change in Congo Basin: Deforestation, reforestation, degradation and regeneration for the years 1990, 2000 and 2005. *Global Change Biology*, *19*(4), 1173–1187.

Eva, H. D., Achard, F., Beuchle, R., De Miranda, E., Carboni, S., Seliger, R., et al. (2012). Forest cover changes in tropical South and Central America from 1990 to 2005 and related carbon emissions and removals. *Remote Sensing*, *4*(5), 1369–1391.

FAO (2006). Global forest resources assessment 2005: Progress towards sustainable forest management. *Food and Agriculture Organization, Rome, FAO Forestry Paper 147*.

FAO (2010). *Global forest resources assessment 2010 main report*. FAO.

Feng, M., Huang, C., Sexton, J. O., Channan, S., Narasimhan, R., & Townshend, J. R. (2012). An approach for quickly labeling land cover types for multiple epochs at globally selected locations. *Geoscience and Remote Sensing Symposium (IGARSS), 2012 IEEE International* (pp. 6203–6206), http://dx.doi.org/10.1109/IGARSS.2012.6352674.

Fortier, J., Rogan, J., Woodcock, C. E., & Miller Runfola, D. (2011). Utilizing temporally invariant calibration sites to classify multiple dates and types of satellite imagery. *Photogrammetric Engineering and Remote Sensing*, *77*(2), 181–189.

Gibbs, H. K., Ruesch, A. S., Achard, F., Clayton, M. K., Holmgren, P., Ramankutty, N., et al. (2010). Tropical forests were the primary sources of new agricultural land in the 1980s and 1990s. *Proceedings of the National Academy of Sciences*, *107*(38), 16732–16737.

Gong, P., Wang, J., Yu, L., Zhao, Y., Zhao, Y., Liang, L., et al. (2013). Finer resolution observation and monitoring of global land cover: First mapping results with Landsat TM and ETM+ data. *International Journal of Remote Sensing*, *34*(7), 2607–2654.

Gray, J., & Song, C. (2013). Consistent classification of image time series with automatic adaptive signature generalization. *Remote Sensing of Environment*, *134*, 333–341.

Gutman, G., Byrnes, R., MASEK, I., Covington, S., Justice, C., Franks, S., et al. (2008). Towards monitoring changes at a Globa the Global Land S. *Photogrammetric Engineering and Remote Sensing*, *74*(1), 6–10.

Hansen, M. C., DeFries, R. S., Townshend, J. R., & Sohlberg, R. (2000). Global land cover classification at 1 km spatial resolution using a classification tree approach. *International Journal of Remote Sensing*, *21*(6–7), 1331–1364.

Hansen, M. C., Potapov, P. V., Moore, R., Hancher, M., Turubanova, S. A., Tyukavina, A., et al. (2013). High-resolution global maps of 21st-century forest cover change. *Science*, *342*(6160), 850–853.

Hansen, M. C., Stehman, S. V., & Potapov, P. V. (2010). Quantification of global gross forest cover loss. *Proceedings of the National Academy of Sciences*, *107*(19), 8650–8655.

Hansen, M. C., Stehman, S. V., Potapov, P. V., Arunarwati, B., Stolle, F., & Pittman, K. (2009). Quantifying changes in the rates of forest clearing in Indonesia from 1990 to 2005 using remotely sensed data sets. *Environmental Research Letters*, *4*(3), 034001.

Herold, M., Mayaux, P., Woodcock, C. E., Baccini, A., & Schmullius, C. (2008). Some challenges in global land cover mapping: An assessment of agreement and accuracy in existing 1 km datasets. *Remote Sensing of Environment*, *112*(5), 2538–2556.

Huang, C., Thomas, N., Goward, S. N., Masek, J. G., Zhu, Z., Townshend, J. R., et al. (2010a). Automated masking of cloud and cloud shadow for forest change analysis using Landsat images. *International Journal of Remote Sensing*, *31*(20), 5449–5464.

Huang, C., Goward, S. N., Masek, J. G., Thomas, N., Zhu, Z., & Vogelmann, J. E. (2010b). An automated approach for reconstructing recent forest disturbance history using dense Landsat time series stacks. *Remote Sensing of Environment*, *114*(1), 183–198.

Kanninen, M., Murdiyarso, D., Seymour, F., Angelsen, A., Wunder, S., & German, L. (2007). Do trees grow on money. The implications of deforestation research for policies to promote REDD. *Forest Perspectives*, *4*.

Kim, D. H., Narashiman, R., Sexton, J. O., Huang, C., & Townshend, J. R. (2011, July). Methodology to select phenologically suitable Landsat scenes for forest change detection. *Geoscience and Remote Sensing Symposium (IGARSS), 2011 IEEE International* (pp. 2613–2616). IEEE.

Lambin, E. F., Geist, H. J., & Lepers, E. (2003). Dynamics of land-use and land-cover change in tropical regions. *Annual Review of Environment and Resources*, *28*(1), 205–241.

Loman, J. O. (2010). *Swedish statistical yearbook of forestry 2010.* Jönköping, Sweden: Swedish Forest Agency.

Loveland, T. R., Reed, B. C., Brown, J. F., Ohlen, D. O., Zhu, Z., Yang, L. W. M. J., et al. (2000). Development of a global land cover characteristics database and IGBP DISCover from 1 km AVHRR data. *International Journal of Remote Sensing*, *21*(6–7), 1303–1330.

Masek, J. G., Huang, C., Wolfe, R., Cohen, W., Hall, F., Kutler, J., et al. (2008). North American forest disturbance mapped from a decadal Landsat record. *Remote Sensing of Environment*, *112*(6), 2914–2926.

Masek, J. G., Vermote, E. F., Saleous, N. E., Wolfe, R., Hall, F. G., Huemmrich, K. F., et al. (2006). A Landsat surface reflectance dataset for North America, 1990–2000. *IEEE Geoscience and Remote Sensing Letters*, *3*(1), 68–72.

Mayaux, P., Holmgren, P., Achard, F., Eva, H., Stibig, H. J., & Branthomme, A. (2005). Tropical forest cover change in the 1990s and options for future monitoring. *Philosophical Transactions of the Royal Society, B: Biological Sciences*, *360*(1454), 373–384.

Mayaux, P., Pekel, J. F., Desclée, B., Donnay, F., Lupi, A., Achard, F., et al. (2013). State and evolution of the African rainforests between 1990 and 2010. *Philosophical Transactions of the Royal Society, B: Biological Sciences*, *368*(1625), 20120300.

McIver, D. K., & Friedl, M.A. (2002). Using prior probabilities in decision-tree classification of remotely sensed data. *Remote Sensing of Environment*, *81*(2), 253–261.

Nepstad, D., McGrath, D., Stickler, C., Alencar, A., Azevedo, A., Swette, B., et al. (2014). Slowing Amazon deforestation through public policy and interventions in beef and soy supply chains. *Science*, *344*(6188), 1118–1123.

Olander, L. P., Gibbs, H. K., Steininger, M., Swenson, J. J., & Murray, B. C. (2008). Reference scenarios for deforestation and forest degradation in support of REDD: A review of data and methods. *Environmental Research Letters*, *3*(2), 025011.

Olson, D. M., Dinerstein, E., Wikramanayake, E. D., Burgess, N. D., Powell, G. V., Underwood, E. C., et al. (2001). Terrestrial ecoregions of the world: A new map of life on Earth a new global map of terrestrial ecoregions provides an innovative tool for conserving biodiversity. *BioScience*, *51*(11), 933–938.

Pan, Y., Chen, J. M., Birdsey, R., McCullough, K., He, L., & Deng, F. (2010). Age structure and disturbance legacy of North American forests. *Biogeosciences Discussions*, *7*(1), 979–1020.

Pax-Lenney, M., Woodcock, C. E., Macomber, S. A., Gopal, S., & Song, C. (2001). Forest mapping with a generalized classifier and Landsat TM data. *Remote Sensing of Environment*, *77*(3), 241–250.

Potapov, P., Yaroshenko, A., Turubanova, S., Dubinin, M., Laestadius, L., Thies, C., et al. (2008). Mapping the world's intact forest landscapes by remote sensing. *Ecology and Society*, *13*(2), 51.

Quinlan, J. R. (1986). Induction of decision trees. *Machine Learning*, *1*(1), 81–106.

Sexton, J. O. (2014). *A model for the propagation of uncertainty from continuous estimates of tree cover to categorical forest cover and change.* Remote Sensing of Environment (in press).

Sexton, J. O., Song, X. P., Feng, M., Noojipady, P., Anand, A., Huang, C., et al. (2013). Global, 30-m resolution continuous fields of tree cover: Landsat-based rescaling of MODIS vegetation continuous fields with lidar-based estimates of error. *International Journal of Digital Earth*, 1–22 (ahead-of-print).

Sexton, J. O., Urban, D. L., Donohue, M. J., & Song, C. (2013). Long-term land cover dynamics by multi-temporal classification across the Landsat-5 record. *Remote Sensing of Environment*, *128*, 246–258.

Sleeter, B.M., Sohl, T. L., Loveland, T. R., Auch, R. F., Acevedo, W., Drummond, M.A., et al. (2013). Land-cover change in the conterminous United States from 1973 to 2000. *Global Environmental Change*, *23*(4), 733–748.

Song, K. (2010). *Tacking uncertainties and errors in the satellite monitoring of forest cover change.* PhD thesis. University of Maryland College Park.

Souza, C. M., Jr., Siqueira, J. V., Sales, M. H., Fonseca, A. V., Ribeiro, J. G., Numata, I., et al. (2013). Ten-year Landsat classification of deforestation and forest degradation in the Brazilian Amazon. *Remote Sensing*, *5*(11), 5493–5513.

Stehman, S. V., Wickham, J.D., Smith, J. H., & Yang, L. (2003). Thematic accuracy of the 1992 National Land-Cover Data for the eastern United States: Statistical methodology and regional results. *Remote Sensing of Environment*, *86*(4), 500–516, http://dx.doi.org/10.1016/S0034-4257(03)00128-7.

Stibig, H. J., Achard, F., Carboni, S., Raši, R., & Miettinen, J. (2014). Change in tropical forest cover of Southeast Asia from 1990 to 2010. *Biogeosciences*, *11*(2), 247–258.

Strahler, A. H. (1980). The use of prior probabilities in maximum likelihood classification of remotely sensed data. *Remote Sensing of Environment*, *10*(2), 135–163.

Thomas, N. E., Huang, C., Goward, S. N., Powell, S., Rishmawi, K., Schleeweis, K., et al. (2011). Validation of North American forest disturbance dynamics derived from Landsat time series stacks. *Remote Sensing of Environment*, *115*(1), 19–32, http://dx.doi.org/10.1016/j.rse.2010.07.009.

Townshend, J. R. (1992). *Improved global data for land applications. A proposal for a new high resolution data set.* Sweden: Report of the Land Cover Working Group of IGBP-DIS. Global Change Report.

Townshend, J. R. G., & Justice, C. O. (1988). Selecting the spatial resolution of satellite sensors required for global monitoring of land transformations. *International Journal of Remote Sensing*, *9*(2), 187–236.

Townshend, J. R., Masek, J. G., Huang, C., Vermote, E. F., Gao, F., Channan, S., et al. (2012). Global characterization and monitoring of forest cover using Landsat data: Opportunities and challenges. *International Journal of Digital Earth*, *5*(5), 373–397.

UNFCCC (2002). Report of the conference of the parties on its seventh session, held at Marrakesh from 29 October to 10 November 2001 [the Marrakesh Accords & the Marrakesh Declaration]. *Addendum part two: Action taken by the conference of parties. Marrakesh, Morocco, 2002.*

Woodcock, C. E., Allen, R., Anderson, M., Belward, A., Bindschadler, R., Cohen, W., et al. (2008). Free access to Landsat imagery. *Science (New York, N.Y.)*, *320*(5879), 1011.

Woodcock, C. E., Macomber, S. A., Pax-Lenney, M., & Cohen, W. B. (2001). Monitoring large areas for forest change using Landsat: Generalization across space, time and Landsat sensors. *Remote Sensing of Environment*, *78*(1), 194–203.

Ylitalo, E. (2010). *Finnish statistical yearbook of forestry.* Vantaa: Metla—Finnish Forest Research Institute.